0026-895X/08/7303-995–1004$20.00
MOLECULAR PHARMACOLOGY
Copyright © 2008 The American Society for Pharmacology and Experimental Therapeutics
Mol Pharmacol 73:995–1004, 2008

Vol. 73, No. 3
41707/3311498
Printed in U.S.A.

Direct Role of Streptozotocin in Inducing Thermal Hyperalgesia by Enhanced Expression of Transient Receptor Potential Vanilloid 1 in Sensory Neurons

Reddy M. Pabbidi, De-Shou Cao, Arti Parihar, Mary E. Pauza, and Louis S. Premkumar

Department of Pharmacology, Southern Illinois University School of Medicine, Springfield, Illinois (R.M.P., D.-S.C., A.P., L.S.P.); and Department of Medical Microbiology, Immunology and Cell Biology & Department of Internal Medicine/Endocrinology, Metabolism and Molecular Medicine, Southern Illinois University School of Medicine Springfield, Illinois (M.E.P.)

Received September 7, 2007; accepted December 14, 2007

ABSTRACT

Streptozotocin (STZ) is a diabetogenic agent extensively used to induce diabetes and to study complications including diabetic peripheral neuropathy (DPN). While studying the influence of transient receptor potential vanilloid 1 (TRPV1) on DPN in the STZ-induced diabetic mouse model, we found that a proportion of STZ-treated mice was nondiabetic but still exhibited hyperalgesia. To understand the mechanism underlying this phenomenon, dorsal root ganglion (DRG) neurons and stably TRPV1 expressing human embryonic kidney (HEK) 293T cells were used to study the expression and function of TRPV1. Incubation of DRG neurons with STZ resulted in a significant increase in the amplitude of capsaicin-induced TRPV1-mediated current and Ca^{2+} influx compared with vehicle-treated sister cultures. It was also found that STZ treatment induced higher levels of reactive oxygen species, which was abolished with concomitant treatment with catalase. Treatment of cells with H_2O_2 mimicked the effects of STZ. Western blot analysis revealed an increase in TRPV1 protein content and phospho p38 (p-p38) mitogen-activated protein kinase (MAPK) levels in DRG of STZ-injected diabetic and nondiabetic hyperalgesic mice compared with control mice. Furthermore, in stably TRPV1-expressing HEK 293T cells, STZ treatment induced an increase in TRPV1 protein content and p-p38 MAPK levels, which was abolished with concomitant treatment with catalase or p38 MAPK inhibitor. These results reveal that STZ has a direct action on neurons and modulates the expression and function of TRPV1, a nociceptive ion channel that is responsible for inflammatory thermal pain.

STZ, a glucosamine-nitrosourea compound obtained from *Streptomyces achromogenes,* is used as a common tool to induce insulin-dependent diabetes mellitus in rodents to study diabetes-induced complications. One such complication is diabetic peripheral neuropathy (DPN). DPN in rodents and humans is characterized by an early thermal and mechanical hyperalgesia (Courteix et al., 1996; Sugimoto et al., 2000). A direct effect of hyperglycemia contributing to hyperalgesia has been suggested by various studies (Courteix et al., 1996; Chen and Pan, 2002). However, treatment with insulin-like growth factor or direct neuronal delivery of low doses of insulin, insufficient to reduce hyperglycemia, ameliorated diabetic neuropathy suggesting that mechanisms other than hyperglycemia may be involved in the pathogenesis of hyperalgesia (Zhuang et al., 1997; Brussee et al., 2004).

STZ is transported into β cells of the pancreas through glucose transporter GLUT2 and causes DNA damage either by alkylation, by the generation of nitric oxide (NO), or by the generation of peroxynitrite (Turk et al., 1993; Schnedl et al., 1994; Kröncke et al., 1995). The DNA strand breaks lead to the activation of the nuclear enzyme poly(ADP-ribose) polymerase (PARP), which synthesizes large amounts of the ADP-ribose polymer, using cellular nicotinamide adenine dinucleotide (NAD^+) as a substrate (LeDoux et al., 1988; Delaney et al., 1995; Pieper et al., 1999). A decrease in the intracellular NAD^+ levels causes a depletion of ATP, a mechanism that can induce cell death (Berger, 1985). Failure of STZ to induce diabetes in PARP-deficient mice suggests the

This work was supported by a National Institutes of Health grant (DK065742) and SIU Excellence in Academic Medicine grant (to L.S.P.).
R.M.P. and D.-S.C. contributed equally to this work.
Article, publication date, and citation information can be found at http://molpharm.aspetjournals.org.
doi:10.1124/mol.107.041707.

ABBREVIATIONS: STZ, streptozotocin; DPN, diabetic peripheral neuropathy; DRG, dorsal root ganglion; FDA, fluorescein diacetate; HA, hemagglutinin; HEK, human embryonic kidney; PWL, paw withdrawal latency; PI, propidium iodide; PARP, poly(ADP-ribose) polymerase; ROS, reactive oxygen species; MAPK, mitogen-activated protein kinase; AM, acetoxymethyl ester; TRPV1, transient receptor potential vanilloid 1; DCF-DA, 2′,7′-dichlorofluorescein diacetate; NGF, nerve growth factor; SB203580, 4-(4-fluorophenyl)-2-(4-methylsulfinylphenyl)-5-(4-pyridyl)1*H*-imidazole.

important role played by PARP in STZ-induced β cell necrosis (Burkart et al., 1999). Another proposed mechanism of STZ-induced cytotoxic effect is its selective inhibition of *N*-acetyl-β-D-glucoaminidase, which is highly expressed in pancreatic β cells compared with neurons (Konrad et al., 2001). Inhibition of *N*-acetyl-β-D-glucoaminidase results in increased glycosylation of proteins, altering their structure and function and leading to the death of β cells (Konrad et al., 2001). In pancreatic β cells, STZ has been shown to produce superoxide anion by inhibiting the Krebs cycle, which will limit the generation of ATP, promoting the death of β cells (Nukatsuka et al., 1990; Sofue et al., 1991; Turk et al., 1993). However, although the effects of STZ are believed to be specific to pancreatic β cells, STZ administration has been shown to adversely affect renal, hepatic, and muscle tissues (Petzold and Swenberg, 1978; Brambilla et al., 1987; Johnston et al., 2007).

Topical application of capsaicin, a transient receptor potential vanilloid 1 (TRPV1) agonist, improves sensory perception in humans with DPN (Forst et al., 2002). In animal models of diabetes, in which DPN manifests as hyperalgesia, TRPV1 expression and function have been shown to be increased (Kamei et al., 2001; Hong and Wiley, 2005). The TRP family of ion channels is involved in sensing physical and chemical stimuli (Clapham, 2003). TRPV1 is a Ca^{2+}-permeant nonselective cation channel expressed predominantly in unmyelinated C fibers and thinly myelinated Aδ fibers (Julius and Basbaum, 2001). TRPV1 is activated by heat (>42°C), capsaicin, protons, *N*-arachidonyl dopamine, anandamide, and leukotrienes (Caterina et al., 1997; Julius and Basbaum, 2001). A role of TRPV1 beyond that of a simple temperature sensor is suggested by the diversity of its agonists and its expression in areas that are not subjected to higher temperatures (Mezey et al., 2000; Birder et al., 2001; Huang et al., 2002). Sensitization of TRPV1 by phosphorylation is mediated by numerous agents, including prostaglandins, bradykinin, glutamate, serotonin, histamine, ATP, and trypsin (Julius and Basbaum, 2001). Modulation by substances associated with inflammation suggests that TRPV1 functions as a sensor of nociceptive inflammatory thermal pain, and the finding is corroborated by a lack of thermal hyperalgesia in TRPV1 knockout mice (Caterina et al., 2000; Davis et al., 2000).

This study was undertaken based on the observation that a proportion of STZ-injected mice did not become diabetic but exhibited hyperalgesia. Here, we sought to determine whether STZ can exert a direct effect on neurons contributing to the hyperalgesia by altering the expression and function of TRPV1.

Materials and Methods

Induction of Diabetes. All procedures used in this study were approved by the animal care and use committee at Southern Illinois University, School of Medicine, and conformed according to National Institutes of Health and institutional guidelines. Mice were housed in standard cages and maintained on a 12-h light/dark cycle at an ambient temperature of 22 ± 1°C. Mice were housed in specific pathogen-free barrier animal facility, and rodent laboratory chow (Laboratory Diet 5001; Nutrition International, Inc., Brentwood, MO) and drinking water were provided ad libitum. Mice were at least 6 to 10 weeks of age and weighed between 18 and 23 g at the beginning of the experiments.

Age-matched single transgenic mice (Ins-HA.D2 mice), which express influenza hemagglutinin (HA) peptide, were used and were kindly provided by Dr. Lo (Lo et al., 1992). Freshly prepared STZ (50–200 mg/kg) in saline (pH 4.5 with 0.1 N citrate buffer) was injected intraperitoneally as described previously (Kamei et al., 1991). Control mice received citrate buffered saline alone. Although Ins-HA.D2 mice are genetically altered, HA expression does not seem to affect glucose metabolism or neuronal function as measured by blood glucose levels and hot plate tests compared with normal wild-type mice.

Glucose levels were determined with an OneTouch Ultra blood glucose monitoring system (LifeScan, Milpitas, CA) using whole blood obtained from the tail. Diabetes was defined as blood glucose concentrations greater than 299 mg/dl (16.7 mM) (Kamei et al., 1991).

Determination of Thermal Pain Sensitivity. All of the mice used in this study were housed in the barrier facility. Mice were tested in the barrier facility on the days the cages were not cleaned to avoid factors that might influence the test measurements. Mice were placed individually on a Hot Plate Analgesia Meter (Harvard Apparatus, Boston, MA) maintained at a constant temperature of 52 ± 0.3°C. The paw withdrawal latency (PWL) is defined as the time taken for the animal to exhibit a distinct pain behavior either by a hind paw lick or a characteristic hind paw flick (whichever occurs first). Mice that did not respond within 20 s were removed from the hot plate to prevent tissue damage. We did not find a significant difference in PWL with either the duration or habituation (0.5–2 h). The experiments were conducted in a blind fashion by measuring the PWL in randomly chosen animals from diabetic or control groups. After completing the test, the ear tags were read to place them in the appropriate groups. There were slight gender differences, but they were not statistically significant, therefore male and female mice were grouped together for further analyses.

In Vitro STZ Treatment. To assess the effect of STZ on TRPV1 expression, reactive oxygen species (ROS) production, or cell viability, cultured DRG neurons and stably TRPV1-expressing HEK 293T cells (Puntambekar et al., 2005) were exposed to 10, 40, 100, 300, 400, and 1000 μM STZ. STZ was prepared as a fresh stock solution by dissolving it in 0.1 N citrate buffer, pH 4.5, before adding it to the neuronal medium and incubated for 24 to 72 h. In the experiments that required the exposure of STZ longer than 24 h, the medium was replaced with appropriated doses of STZ. The experimental observations were compared with sister cultures that were treated with 0.1 N citrate buffer.

Electrophysiology. Primary DRG neuronal cultures were prepared from embryonic day 18 rat embryos. Adult pregnant rats were killed with an overdose of isoflurane. DRG were dissected, and the neurons were dissociated by trituration with a fire-polished glass pipette in Hanks' balanced salt solution (Ca^{2+}- and Mg^{2+}-free). Neurons were cultured in neurobasal medium (Invitrogen, Carlsbad, CA), supplemented with L-glutamine and B27 supplement (Invitrogen, Grand Island, NY) and grown on poly(D-lysine)-coated glass coverslips in 24-well plates. Neurons were incubated at 37°C in a humidified atmosphere of 5% CO_2. Neurons were used from 3 days after plating.

For whole-cell patch clamp current recordings, the bath solution contained 140 mM sodium gluconate, 2.5 mM KCl, 10 mM HEPES, 1 mM $MgCl_2$, and 1.5 mM EGTA, with pH adjusted to 7.35 with NaOH, and the pipette solution contained 140 mM potassium gluconate, 5 mM KCl, 10 mM HEPES, 2 mM $MgCl_2$, 10 mM EGTA, 2 mM ATP, and 0.25 mM GTP, with pH adjusted to 7.35 with NaOH. Ca^{2+}-free extracellular solution was used to avoid desensitization and tachyphylaxis of capsaicin-induced currents. The junction potential between the patch pipette and the bath solutions was cancelled before the gigaohm seal was formed. The tip of the drug application pipettes was placed within 100 μm of the neurons. Currents were recorded using a WPC-100 patch-clamp amplifier (E.S.F. Electronic, Goettingan, Germany). Data were digitized (VR-10B; InstruTech, Great Neck, NY) and stored in videotapes or directly stored in the computer using a Lab View (National Instruments, Austin, TX) interface. For analysis, data were filtered at 2.5 kHz (−3 dB fre-

quency with an eight-pole low-pass Bessel filter, LPF-8; Warner Instruments, Hamden, CT) and digitized at 5 kHz. Current amplitudes were measured using Channel 2 Software (kindly provided by Michael Smith, Australian National University, Canberra, Australia). The traces and graphs were plotted using Origin Software (OriginLab Corp., Northampton, MA). Capacitance of the cell was measured manually by using the readout in the WPC-100 amplifier.

Measurement of ROS. ROS production was detected using the dye 2′,7′-dichlorofluorescein diacetate (DCF-DA; Invitrogen). DCF-DA, a nonfluorescent cell-permeant compound, is cleaved by endogenous esterases and the de-esterified product becomes fluorescent upon oxidation by ROS. Cells were incubated with DCF-DA (20 μM) at 37°C for 20 min and washed twice in Hanks' balanced salt solution to reduce nonspecific fluorescence. Fluorescence measurements were carried out using an inverted microscope (DMIRE2; Leica, Plymouth, MN) equipped with a camera (Retiga Ex; Roper Scientific, Ottobrunn, Germany) and the Lambda DG4 wavelength switcher (Sutter Instrument Company, Novato, CA), and the data were analyzed using Scanalytics software (Scanalytics Inc., Fairfax, VA). The exposure time was kept to <1 s to avoid photo oxidation of the ROS-sensitive dyes, and for all treatments, the exposure time was kept constant. At least three independent fields were chosen for each condition, and 5 to 20 cells in a given field were used for quantification of the fluorescence signals. DCF fluorescence was measured and collected with an excitation (λ_{exc}) of 488 nm and emission (λ_{emi}) of 535 nm.

Ca^{2+} Imaging. DRG neurons grown on glass coverslips were incubated with Fluo-4 AM (3 μM) (Invitrogen) for 20 min at 37°C and washed with physiological buffer containing 140 mM NaCl, 5 mM HEPES, 2 mM $CaCl_2$, 1 mM $MgCl_2$, 2.5 mM KCl, and 2 mM lidocaine, pH 7.35. The experiments were carried out using a microscope (DMIRE2) attached to a camera (Retiga Ex), and the Lambda DG4 wavelength switcher (Sutter Instruments). Fluo-4 was excited at 488 nm, and the emitted fluorescence was filtered with a 535 ± 25 nm bandpass filter and analyzed using the Scanalytics software. Multiple cells were selected, and the fluorescence of individual cells was tracked. The ratio of the fluorescence change F/F_o was plotted to represent the change in intracellular Ca^{2+} levels.

Cell Viability Assay. Coverslips containing embryonic DRG neurons were incubated with 15 μl of fluorescein diacetate (FDA; 15 mg/ml) and 15 μl of propidium iodide (PI; 4.6 mg/ml) for 3 min by adding them into 0.5 ml of neurobasal medium. Cells were washed twice with Ca^{2+}-free buffer to prevent nonspecific background fluorescence. Green fluorescence (λ_{exc} 488 nm and λ_{emi} 520 nm wavelengths for FDA) for live and red fluorescence (λ_{exc} 535 nm and λ_{emi} 590–615 nm wavelengths for PI) for dead cells were observed using a microscope (DMIRE2) equipped with a camera (Retiga Ex) and the Lambda DG4 wavelength switcher (Sutter Instruments) and were analyzed using Scanalytics software. At least five to six independent fields were chosen for analysis for each condition. The percentage of survival or viability of DRG neurons was calculated for different concentrations of STZ.

Western Blot. Mice were sacrificed 1 week after STZ treatment, and DRG were removed and placed in a lysis buffer (0.1% SDS, 1% Triton X-100, 1% deoxycholate, protease, and phosphatase inhibitor cocktail, 1:100; Sigma, St. Louis, MO), homogenized, and centrifuged. Stably TRPV1-expressing HEK 293T cells were cultured as described previously (Puntambekar et al., 2005). TRPV1-expressing HEK cells were scraped into a 400-μl lysis buffer and centrifuged. The protein concentration was measured by the bicinchoninic acid assay. Proteins were separated by 10% SDS-polyacrylamide gel electrophoresis and transferred to the nitrocellulose membrane (Bio-Rad Laboratories, Hercules, CA). Membranes were probed overnight with rabbit anti-p38, phospho-p38 (1:200; Santa Cruz Biotechnology, Santa Cruz, CA), β-Actin (1:200; Sigma), or goat anti-TRPV1 (1:100; Santa Cruz Biotechnology) antibodies followed by incubation with horseradish peroxidase-conjugated goat anti-rabbit IgG or rabbit anti-goat IgG (1:10,000, Santa Cruz Biotechnology) for 1 h. After incubation with enhanced chemiluminescence reagents (Santa Cruz Biotechnology), membranes were scanned using the Hitachi genetic systems (Hitachi Software Engineering, Tokyo, Japan), and blots were analyzed using GeneTools Analysis Software (SynGene, Frederick, MD).

Data Analysis. For behavioral experiments, mixed model analysis was performed using SAS/STAT software (SAS Institute, Cary, NC), which included both fixed events (age and time after diabetes onset) and random events (number of subjects) with repeated measures of analysis of variance. The comparisons were made between control group and diabetic groups. Data are shown as mean ± S.E.M.. Data are considered significant at $p < 0.05$. For all other experiments, data are shown as mean ± S.E.M. Significance is tested using unpaired Student's t test, and the data are considered significant at $p < 0.05$. DCF and Fluo-4 AM were obtained from Invitrogen. B27-supplement was obtained from Invitrogen. p38 MAPK inhibitor SB203580 was obtained from Santa Cruz Biotechnology. All other chemicals used in this study were obtained from Sigma.

Results

Alterations in Thermal Pain Sensitivity in STZ-Injected Diabetic Mice. STZ is commonly used to induce type 1 diabetes in rodents for the study of DPN because disease induction is both rapid and reliable. In this study, we observed the STZ-treated mice for a period of 7 to 9 weeks after the onset of diabetes. Ins-HA.D2 single transgenic mice were injected with a single dose of STZ (200 mg/kg). After STZ treatment, blood glucose levels were significantly elevated (70–75% of the mice) by the first week after treatment and remained elevated for the course of the study (preinjection, 157 ± 4.4; week 1 STZ, 503.5 ± 24.6; week 7 STZ, 574.7 ± 22.6 mg/dl, $n = 11$) compared with control vehicle-injected mice (preinjection, 157 ± 6.1; week 1 control, 183.6 ± 2.2; week 7 control, 170 ± 2 mg/dl, $n = 6$, $p < 0.001$) (Fig. 1A). As the disease progressed, the body weights of STZ-treated animals remained stagnant, whereas the body weights of control animals increased steadily (STZ week 1, 22.9 ± 0.5; STZ week 6, 21.2 ± 0.6, g, $n = 11$, $p < 0.001$; control week 1, 22.1 ± 0.2; control week 6, 26.2 ± 0.3 g, $n = 6$) (Fig. 1B).

Then the mice were tested for thermal pain sensitivity by measuring the PWL using a hot plate maintained at 52 ± 0.3°C. An early phase of thermal hyperalgesia occurred between 1 and 3 weeks after STZ treatment, which paralleled the onset of hyperglycemia (control week 2, 8.9 ± 0.5 s, $n = 19$; diabetic week 2, 7.1 ± 0.4 s, $n = 33$, $p < 0.001$) (Fig. 1C). Hyperalgesia was followed by a phase of hypoalgesia (control week 8, 9 ± 0.8 s, $n = 19$, diabetic week 8, 13.4 ± 0.7 s, $n = 8$, $p < 0.001$) (Fig. 1C). Together these results indicate that STZ-induced diabetic mice exhibited an initial phase of hyperalgesia followed by a phase of hypoalgesia.

Alterations in Thermal Pain Sensitivity in STZ-Injected Nondiabetic Mice. A proportion (20–25%) of STZ-injected mice did not become diabetic as indicated by the blood sugar levels (<300 mg/dl), but these mice exhibited thermal hyperalgesia. This was further confirmed by a nondiabetogenic dose of STZ (50 mg/kg). The blood glucose levels were slightly higher compared with vehicle-injected mice (STZ-injected nondiabetic mice, 170 ± 8.8; week 2, 222.4 ± 24.3; week 6, 211.4 ± 19.6 mg/dl, $n = 13$; vehicle-injected mice, 157 ± 6.1; week 2, 163.8 ± 3.9; week 6, 186 ± 1.6 mg/dl, $n = 6$) (Fig. 2A). Body weights of STZ-injected nondiabetic and vehicle-injected mice increased steadily (STZ-injected nondiabetic mice week 1, 23 ± 1; and week 6, 25.2 ± 0.9 g,

$n = 13$) (vehicle-injected mice week 1, 22.1 ± 0.2; week 6, 26.2 ± 0.3 g, $n = 6$) (Fig. 2B). STZ-injected nondiabetic mice exhibited a phase of hyperalgesia (STZ-injected nondiabetic mice, 9.6 ± 0.5 s; week 2, 6.1 ± 0.3 s, $n = 13$; $p < 0.001$) followed by a phase of normal PWL (STZ-injected nondiabetic mice week 7, 7.9 ± 0.6 s, $n = 13$; vehicle-injected mice, week 8, 9 ± 0.8 s, $n = 6$) (Fig. 2C). These results suggest that STZ treatment induces changes in thermal pain sensitivity, which is independent of hyperglycemia.

Incubation of Neurons with STZ Increases TRPV1-Mediated Current Responses. To determine whether STZ has a direct action on neurons, cultured embryonic DRG neurons were incubated for 24 h with different concentrations of STZ (20–400 μM), and capsaicin (1 μM)-induced TRPV1-mediated whole-cell currents were recorded. There was a dose-dependent increase in TRPV1 current at lower concentrations followed by a decrease at higher concentrations. Vehicle-treated sister cultures were used as controls. TRPV1-mediated currents were significantly higher at 20 μM (control, 1 ± 0.1, $n = 10$; STZ, 2.0 ± 0.1-fold, $n = 10$, $p < 0.004$) and 100 μM STZ (control, 1 ± 0.1, $n = 9$; STZ, 2.5 ± 0.2-fold, $n = 9$, $p < 0.04$), but there was no significant change at 200 μM STZ (control, 1 ± 0.3, $n = 10$; STZ, 1.1 ± 0.2-fold, $n = 10$), and a decrease in the current amplitude was observed at 400 μM STZ (control, 1 ± 0.2, $n = 6$; STZ, 0.6 ± 0.2-fold, $n = 6$) (Fig. 3B). Typically, small-diameter (<25 μm) neurons responded to capsaicin. Average capacitance of DRG neurons in 100 μM STZ-treated neurons (19.2 ± 1.48 pF, $n = 9$) did not differ from that of control neurons (21.5 ± 1.7 pF, $n = 11$). Peak current amplitudes were expressed as current densities (in picoamperes per picofarads) using cell capacitance to normalize the differences in cell size, which was found to be significantly higher at 20 and 100 μM STZ concentrations (control, 1 ± 0.2, $n = 10$; 20 μM STZ, 1.7 ± 0.2-fold, $n = 10$, $p < 0.004$) (control, 1 ± 0.2, $n = 9$; 100 μM STZ, 2.1 ± 0.2-fold, $n = 9$; $p < 0.05$) but not at 200 and 400 μM STZ (Fig. 3C). These results demonstrate that lower concentrations of STZ (20 and 100 μM) induce an increase in TRPV1-mediated currents, whereas higher concentrations (>200 μM) cause a decrease, possibly as a result of reaching toxic concentrations. Elevated TRPV1 currents may be one of the mechanisms by which neuronal excitability increases, contributing to hyperalgesia observed in STZ-injected diabetic and nondiabetic mice.

To corroborate the finding that the treatment of STZ increases TRPV1 function, increases in intracellular Ca^{2+} in response to application of capsaicin (30 nM) were monitored in cultured DRG neurons loaded with Fluo-4 AM after STZ treatment. The advantage of the Ca^{2+} imaging technique is that it enables the study of multiple neurons at the same time. As described earlier, sister cultures were used in parallel to determine the effect induced by STZ. We observed a significantly higher TRPV1-mediated Ca^{2+} influx in embryonic DRG neurons incubated with STZ (40 μM) for 24, 48, and 72 h (Fig. 4, A and B) compared with sister cultures treated with a citrate buffer (0.1 N) (-fold change in F/F_o: citrate buffer, 1 ± 0. 01, $n = 49$ cells; STZ (40 μM) 24 h, 1.7 ± 0.4, $n = 75$ cells; $p < 0.05$; 48 h, 3.3 ± 0.7, $n = 88$ cells; 72 h, 1.3 ± 0.4, $n = 65$ cells) (Fig. 4C). These results suggest that long-term STZ treatment increases the function of TRPV1

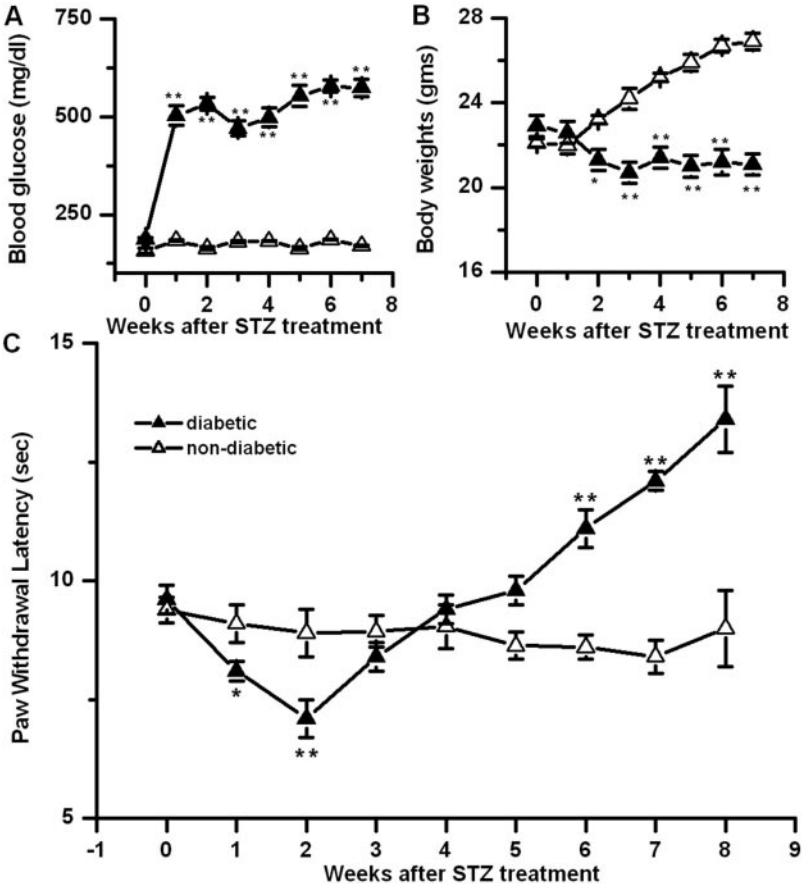

Fig. 1. Altered thermal pain sensitivity in STZ-induced diabetic mice. A, blood glucose levels were significantly higher in diabetic mice (▲) compared with control mice (△). B, the body weight of diabetic mice (▲) remained constant, whereas the body weight of control mice (△) steadily increased. C, diabetic mice (▲) show significant changes in PWL: they exhibited a period of hyperalgesia between weeks 1 and 4 and then a phase of hypoalgesia compared with vehicle-injected mice (△). Asterisks represent the significance levels (*, $p < 0.05$; **, $p < 0.01$).

either by an increase in the membrane expression of TRPV1 or an increase in TRPV1 sensitivity. However, longer exposure to STZ resulted in a decrease in Ca^{2+} influx, possibly as a result of toxicity, as seen with current recordings (Fig. 3).

We noticed a decrease in TRPV1-mediated current when the neurons were exposed to higher concentrations of STZ (>200 μM). Studies have suggested that 1 mM STZ induces pancreatic β cell death in vitro (Nukatsuka et al., 1990; Konrad et al., 2001). Based on these studies, we hypothesized that STZ might alter the viability of DRG neurons. To test whether STZ can alter the viability of neurons, we performed a viability assay using live and dead cell staining dyes FDA

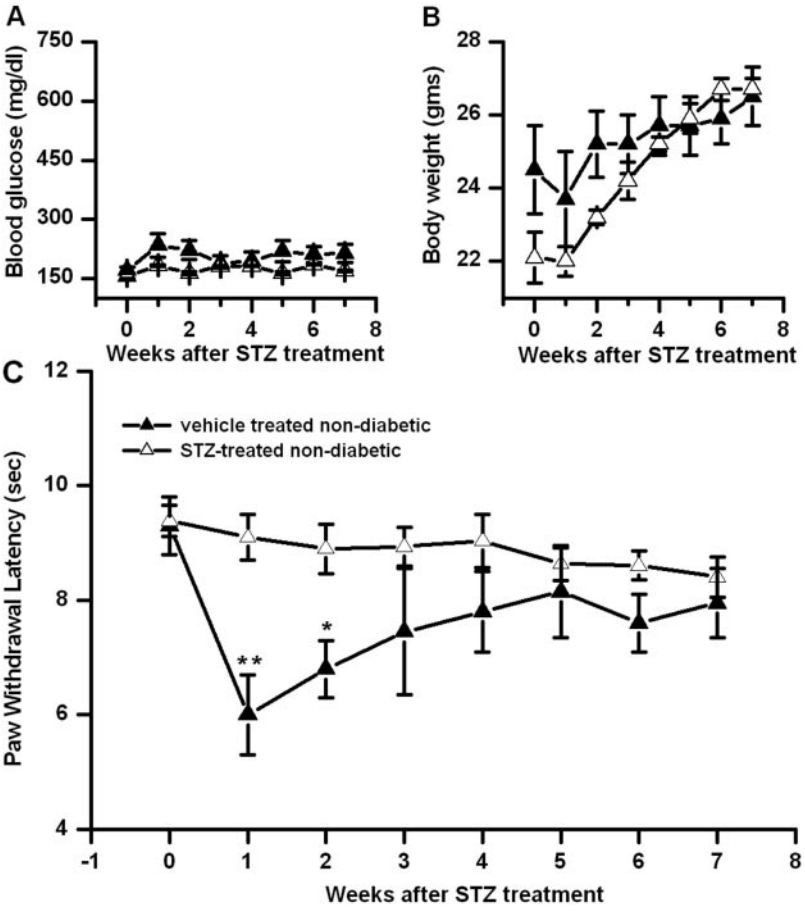

Fig. 2. Altered thermal pain sensitivity in STZ-injected nondiabetic mice. A, a proportion of STZ-injected mice (▲) did not show elevated blood glucose levels and were similar to vehicle-injected mice (△). B, body weights of both STZ-injected nondiabetic mice (▲) and vehicle-injected mice (△) steadily increased. C, STZ-injected nondiabetic mice (▲) exhibited a phase of thermal hyperalgesia compared with vehicle-injected mice (△). Asterisks represent the significance levels (*, $p < 0.05$; **, $p < 0.01$).

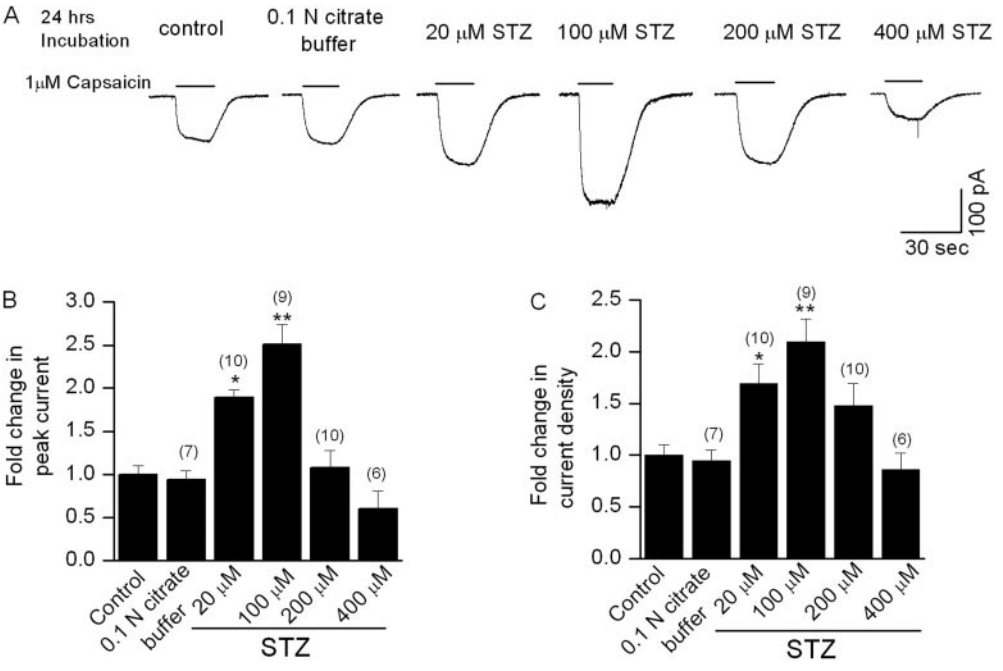

Fig. 3. TRPV1-mediated currents after incubation of cultured DRG neurons with STZ. A, incubation with lower concentrations of STZ (20 and 100 μM) for 24 h increased capsaicin (1 μM)-evoked currents recorded from small- to medium-diameter DRG neurons compared with 0.1 N citrate buffer-treated DRG neuronal sister cultures. But at higher concentrations of STZ (>200 μM), capsaicin-evoked currents decreased. B and C, summary graphs show the -fold change in peak current amplitude and current densities in STZ-treated neurons. The number in parenthesis represents the number of cells, and the asterisks represent the significance levels (*, $p < 0.05$; **, $p < 0.001$ compared with control).

and PI, respectively. Results of the viability assay suggest that increasing concentrations of STZ decreased the viability of embryonic DRG neurons (200 μM, 26%, $n = 180$; 400 μM, 27.4%, $n = 114$; and 1000 μM STZ, 16.4%, $n = 64$, viable cells) compared with vehicle-treated sister cultures.

STZ Treatment Induces ROS Production in Cultured DRG Neurons in Vitro. It has been suggested that short- and long-term treatments of STZ induce myopathy through the ROS-mediated mechanism (Johnston et al., 2007). Likewise, nerve growth factor (NGF) induces TRPV1 expression through NADPH oxidase-dependent ROS pathway (Suzukawa et al., 2000; Puntambekar et al., 2005). Therefore, we determined whether ROS is involved in the STZ-induced increase in TRPV1 currents. Initially, we tested whether a known ROS-generating agent, such as hydrogen peroxide, (H_2O_2, 25 μM) could increase DCF fluorescence intensity in cultured DRG neurons treated for 24 h. As expected, H_2O_2 significantly increased DCF fluorescence (data not shown). Next, to determine the role of STZ, we pretreated the cultured embryonic DRG neurons with different concentrations of STZ for 24 h, and changes in ROS were measured. We observed a higher DCF fluorescence intensity with increasing concentrations of STZ (citrate buffer, 1 ± 0.03, $n = 170$ cells; 100 μM STZ, 1.8 ± 0.04, $n = 105$ cells, $p < 0.0001$; 400 μM STZ, 1.77 ± 0.05, $n = 75$ cells, $p < 0.0001$) (Fig. 5). These results suggest that STZ treatment induces ROS production in cultured DRG neurons, which might play a role in increasing TRPV1-mediated current through ROS-mediated transcriptional or translational regulation. Although ROS levels were higher even at a higher concentration of STZ (400 μM) treatment, TRPV1-mediated currents showed a reduction (Fig. 3), suggesting that higher levels of ROS may become toxic to neurons.

To further test that ROS is involved in STZ-induced TRPV1 expression and function, we pretreated cultured DRG neurons with H_2O_2 (25 μM) for 24 h, and TRPV1-mediated whole-cell currents were recorded. There was a significant increase in TRPV1-mediated currents compared with citrate buffer-treated cells (buffer, 1 ± 0.1-fold, $n = 8$; 25 μM H_2O_2, 1.7 ± 0.1-fold, $n = 8$, $p < 0.05$), whereas treatment with 50 μM H_2O_2, in fact resulted in a decrease in the current amplitude (50 μM H_2O_2, 0.63 ± 0.19-fold, $n = 8$), suggesting a narrow effective range of ROS in modulating TRPV1 responses (Fig. 6, A and B). Peak currents normalized to capacitance (measured in picoamperes per picofarads) were also found to be increased (buffer, 1 ± 0.1-fold, $n = 8$; 25 μM H_2O_2, 2.0 ± 0.1-fold, $n = 8$, $p < 0.002$) (Fig. 6C). To further confirm that ROS is involved in STZ-induced TRPV1 expression, cultured DRG neurons were concomitantly treated with catalase (200 U/ml), a ROS scavenger. TRPV1-mediated whole-cell currents recorded from the neurons incubated with STZ (100 μM) + catalase or H_2O_2 (25 μM) + catalase did not increase the current amplitude (buffer, 1 ± 0.2, $n = 9$; STZ + catalase, 0.96 ± 0.06-fold, $n = 10$; buffer, 1 ± 0.2-fold, $n = 7$; H_2O_2 + catalase, 1.1 ± 0.2-fold, $n = 8$). Peak current amplitudes expressed as current densities (measured in picoamperes per picofarads) were not altered after treatment with catalase (STZ + catalase, 0.94 ± 0.09-fold, $n = 8$; H_2O_2 + catalase, 1.07 ± 0.18-fold, $n = 8$) (Fig. 6, A and B). Average capacitance values of DRG in STZ +catalase-treated neurons (18.5 ± 0.67 pF, $n = 8$) did not differ from control (18.1 ± 0.7 pF, $n = 10$). These data implicate that STZ-induced ROS levels are involved in the increase in TRPV1-mediated current.

Increase in TRPV1 and p-p38 MAPK Levels in Diabetic and Nondiabetic Hyperalgesic Mice. Activation of MAPKs increases the expression of proteins either by transcriptional or post-translational mechanisms. DRG obtained from STZ-treated diabetic or nondiabetic mice 1 week after injection of STZ were probed with TRPV1 and p-p38 MAPK antibodies. Our results demonstrate an increase in TRPV1 levels (expressed as a ratio of β-actin levels) in both diabetic (1.73 ± 0.25-fold; $n = 3$, $p < 0.05$) and nondiabetic hyperalgesic DRG (1.52 ± 0.07-fold, $n = 3$, $p < 0.05$) (Fig. 7) com-

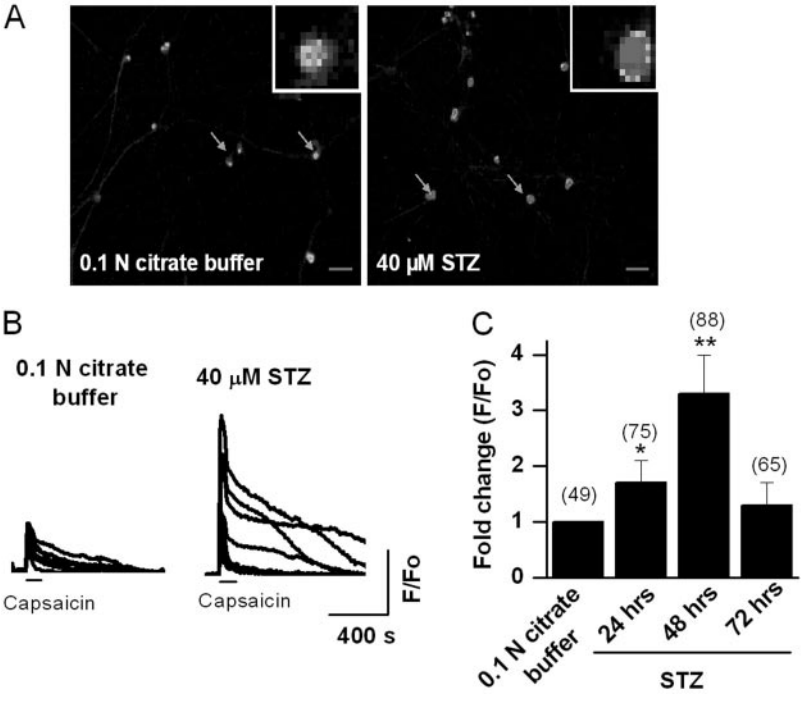

Fig. 4. Treatment of STZ increases TRPV1-mediated Ca^{2+} influx in cultured DRG neurons. Selected DRG neurons in a coverslip were individually tracked for changes in intracellular Ca^{2+} levels in response to application of capsaicin (30 nM) A, representative images showing capsaicin-induced increase in intracellular Ca^{2+} after STZ (40 μM) treatment compared with 0.1 N citrate buffer treatment. The inset shows the enlarged image of one of the neurons pointed with arrows. B, representative traces of changes in fluorescence intensity in a group of STZ-treated neurons (right, $n = 9$) and buffer-treated neurons (left, $n = 11$). C, summary graph depicting the -fold increase in fluorescence intensity (F/F_o) in STZ-treated neurons compared with buffer-treated cultures. Number in the parenthesis represents the number of cells, and the asterisks represent the significance levels (*, $p < 0.05$; **, $p < 0.01$ compared with control). Scale bar, 100 μm.

pared with vehicle-treated mice. In addition, the p-p38 MAPK levels (expressed as a ratio of total p38 MAPK levels) were elevated in STZ-treated diabetic (1.45 ± 0.14-fold; $n = 3$, $p < 0.05$) and nondiabetic hyperalgesic mice (1.43 ± 0.05-fold; $n = 3$, $p < 0.05$) compared with control mice (Fig. 7). Total p38 MAPK levels remained constant after STZ treatment, indicating that STZ caused an increase in the phosphorylation of p38 MAPK rather than increasing the levels of the substrate.

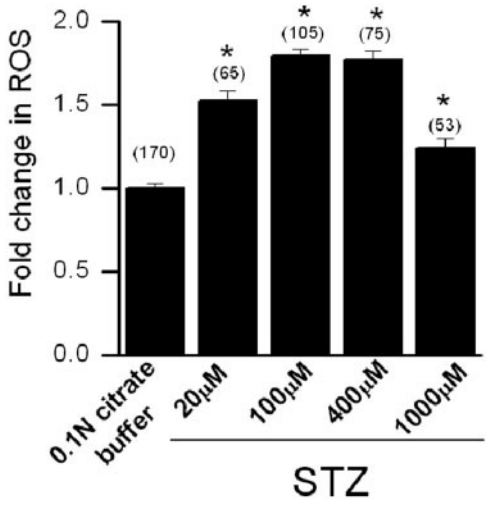

Fig. 5. Generation of ROS after incubation of cells with STZ. STZ- or vehicle-treated DRG neurons for 24 h were preloaded with DCF-DA (20 μM), and DCF fluorescence intensity was measured. Summary graph depicting a significant increase in DCF fluorescence intensity in STZ (20–1000 μM)-treated DRG neurons compared with vehicle-treated neuronal sister cultures. Number in the parenthesis represents the number of DRG neurons, and the asterisk represents significance level (*, $p < 0.001$ compared with control).

Activation of STZ-ROS-p38 MAPK Pathway Promotes TRPV1 Expression. Previous studies have suggested that JNK and p38 MAPK are strongly activated by ROS or by a mild oxidative shift of the intracellular thiol/disulfide redox state (Abe et al., 1996; Hehner et al., 2000). A similar mechanism is also involved in the NGF-induced increase in TRPV1 expression, in which p38 MAPK is activated by ROS, thereby contributing to hyperalgesia (Ji et al., 2002; Puntambekar et al., 2005). Experiments were conducted using stably TRPV1-expressing HEK 293T cells to determine whether the increase in TRPV1 expression induced by long-term STZ treatment is mediated by the ROS-p38 MAPK pathway. Cells were treated with STZ, ROS-generating and -scavenging agents, and then probed for TRPV1 and p-p38 MAPK. Consistent with our previous results, STZ (100 μM)-treated cells exhibited an elevated TRPV1 expression (1.52 ± 0.13-fold, $n = 4$, $p < 0.01$) (Fig. 8B). Removal of ROS by catalase (200 U/ml) abolished this increase (1.08 ± 0.02-fold, $n = 4$, $p < 0.05$). p-p38 MAPK was also found to be increased in STZ-treated cells (1.25 ± 0.04-fold, $n = 4$, $p < 0.01$) but did not increase when treated simultaneously with catalase (0.98 ± 0.04-fold, $n = 4$, $p < 0.05$) (Fig. 8B). In support of our findings, we successfully reproduced these results with a ROS-generating agent, H_2O_2 (25 μM) (TRPV1: H_2O_2, 1.4 ± 0.1-fold, $n = 4$, $p < 0.01$; H_2O_2 + catalase, 1.01 ± 0.09-fold, $n = 4$, $p < 0.05$) (p-p38 MAPK: H_2O_2, 1.48 ± 0.09-fold, $n = 4$, $p < 0.01$; H_2O_2 + catalase, 0.92 ± 0.06-fold, $n = 4$, $p < 0.05$) (Fig. 8C), suggesting that STZ-induced TRPV1 expression is mediated by the ROS-p38 MAPK pathway. To confirm that the effect is mediated by p38 MAPK, we incubated the cells with a p38 MAPK inhibitor, SB203580 (20 μM). The increase in TRPV1 and p-p38 MAPK levels was significantly reduced after treatment with the inhibitor (TRPV1, 1.08 ± 0.11-fold, $n = 3$, $p < 0.05$; p-p38 MAPK, 0.95 ± 0.08-fold, $n = 3$, $p < 0.05$) (Fig. 8D).

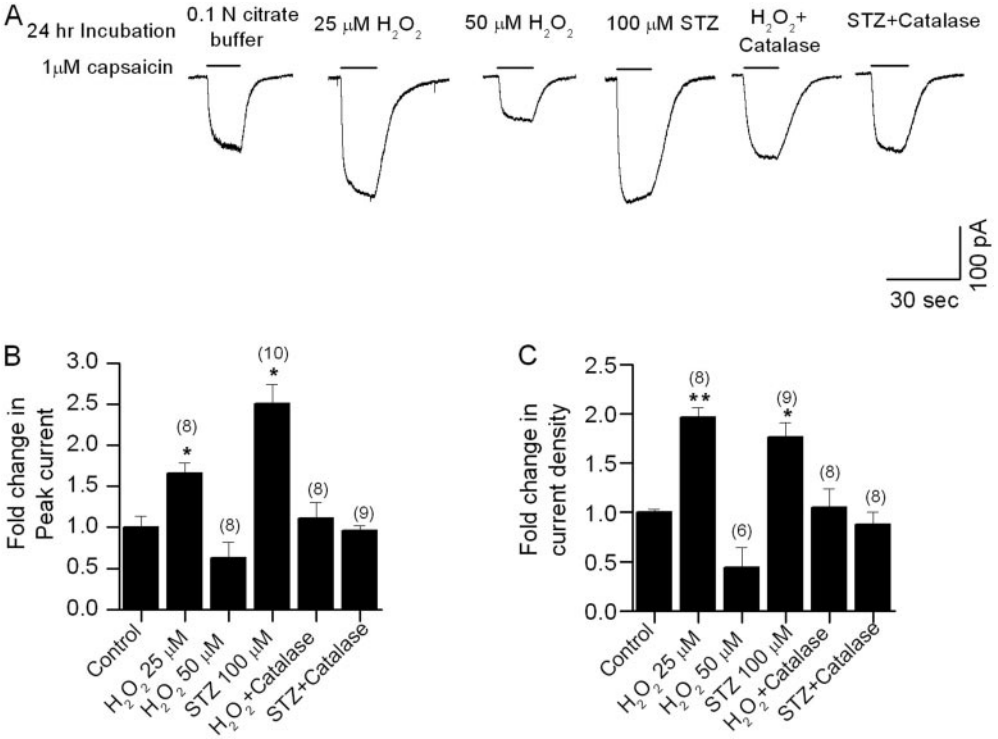

Fig. 6. STZ-induced increase in TRPV1 current is mimicked by H_2O_2 and abolished by concomitant treatment with catalase. A, representative traces show that the incubation of neuronal cultures with ROS generator H_2O_2 (25 μM) increased the capsaicin-evoked current amplitude compared with currents recorded from neurons in sister cultures. Higher concentration of H_2O_2 (50 μM) caused a decrease in current amplitude. The increase in current amplitude induced by STZ and H_2O_2 was reversed by concomitant treatment with catalase. B and C, summary graphs show the change in current amplitude and current densities after incubation of cultures with H_2O_2 or STZ or along with catalase. Asterisks represent the significance levels (*, $p < 0.05$; **, $p < 0.01$ compared with control).

Discussion

STZ is a glucosamine nitrosourea compound with diabetogenic properties purported to cause a selective destruction of pancreatic β cells. STZ-induced diabetic mice exhibit two phases of thermal pain sensitivity: an initial phase of hyperalgesia, and a late phase of hypoalgesia. However, a proportion (~20–25%) of STZ-treated mice did not become diabetic but became hyperalgesic compared with the vehicle-injected group. It was further confirmed that hyperalgesia was observed in nondiabetogenic doses of STZ. However, we could not find a correlation between the degree of hyperalgesia and the dose of STZ. Possible reasons for the failure of STZ to induce diabetes are 1) inability to damage all pancreatic β cells as a result of insufficient concentration; 2) faster recovery of damaged pancreatic β cells; and 3) decreased bioavailability as a result of rapid breakdown by the liver enzymes or rapid excretion by the kidneys. A normal gain of body weight in STZ-injected nondiabetic mice and a decrease in the body weight of diabetic mice suggest that STZ-injected nondiabetic mice do not suffer from metabolic derangement. Both time course and the degree of thermal hyperalgesia were similar in all STZ-treated mice, regardless of their blood glucose levels after STZ injection. Other investigators have not reported this phenomenon, perhaps because of the common practice of excluding nondiabetic mice from studies. However, it has been reported in a study that ~40 to 60% of rats injected with STZ were nondiabetic but exhibited mechanical hyperalgesia and insulinopenia (Romanovsky et al., 2004). It was suggested that insulinopenia itself or consequences of insulinopenia that is independent of hyperglycemia might contribute to mechanical hyperalgesia. A direct effect of STZ was ruled out as a possible causative factor of mechanical hyperalgesia because insulin-treated STZ-injected diabetic rats became normoglycemic and exhibited attenuated pain sensation (Courteix et al., 1996).

TRPV1 plays a role in both diabetic and inflammatory hyperalgesia (Caterina et al., 2000; Hong and Wiley, 2005). STZ destroys pancreatic β cells by elevating the ROS levels (Nukatsuka et al., 1990; Sofue et al., 1991; Turk et al., 1993). In another study, moderate increases in ROS levels have been shown to function as secondary messengers that can influence redox-sensitive signal transduction pathways (Suzukawa et al., 2000). In our in vitro studies, STZ-treated neurons exhibited an increase in TRPV1-mediated currents and an increase in the levels of ROS. By recording TRPV1-mediated whole-cell currents in cultured embryonic DRG neurons treated with ROS-generating and -scavenging agents, we have shown that STZ induces TRPV1 expression through the ROS-mediated pathway. We further observed that STZ also caused an increase in the phosphorylated form of p38 MAPK, suggesting that the increase in the TRPV1 protein expression may involve the ROS-p38 MAPK pathway. However, at higher concentrations of STZ and higher levels of ROS, the effect of toxicity is seen as a decrease in TRPV1 expression and a reduction in cell viability.

Peripheral nerve injury leads to an increase in the expression of brain-derived neurotrophic factor and the $\alpha 2\delta$ Ca^{2+} channel subunit through activation of p38 MAPK (Zhou et al., 1999; Luo et al., 2001). A similar mechanism is also involved in NGF-induced increase in TRPV1 expression, in which p38 MAPK is activated by ROS, thereby contributing to hyperalgesia (Ji et al., 2002; Puntambekar et al., 2005). Ji et al. (2002) have proposed that p38 MAPK activates the translational factor eIF4E via MAPK-interacting kinases 1 and 2 and the phosphorylation of which results in an increased affinity of eIF4E for capped RNA influencing translation. Different oxidative stress-inducing stimuli, such as relatively low concentrations of hydrogen peroxide, UV light, γ-irradiation, and interleukin-1, have been shown to activate the activator protein-1, a transcription factor (Angel and Karin, 1991; Devary et al., 1991; Meyer et al., 1993). Likewise, STZ-ROS-p38 MAPK pathway could increase the activity of transcription factors like activator protein-1, inducing transcription of TRPV1, or it may increase the translation of TRPV1 through elF4E. This could lead to an increase in membrane expression and function of TRPV1, thereby contributing to the hyperalgesia observed in STZ-injected nondiabetic mice. Nevertheless, a similar mechanism cannot be ruled out in STZ-injected diabetic mice. In HEK cells stably transfected with TRPV1, treatment of STZ caused a similar increase in TRPV1 and p-p38 MAPK expression suggesting that the effect we observe is post-translational rather than post-transcriptional.

It has been suggested that STZ is transported into β cells through the glucose transporter GLUT2 (Schnedl et al., 1994). It is intriguing that the predominant glucose transporter expressed in the peripheral nervous system is GLUT3. STZ treatment may result in PARP activation, possibly through its direct damaging effects of DNA. PARP activation results in an increased production of poly(ADP-ribose), from

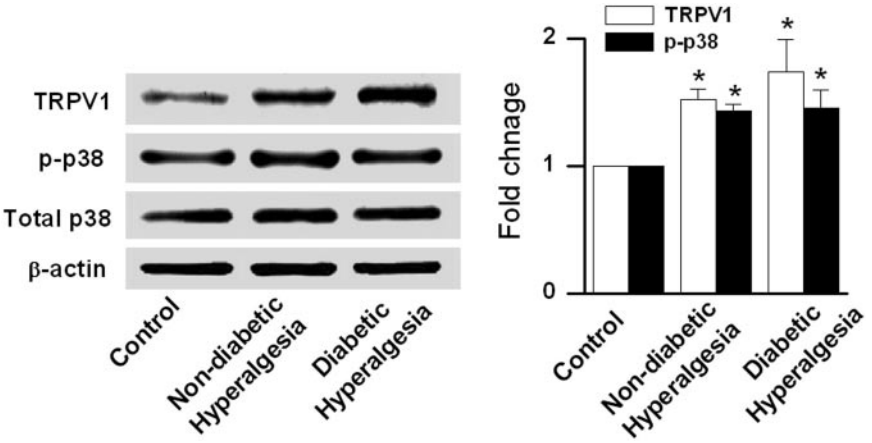

Fig. 7. TRPV1 and p38 MAPK levels in DRG of STZ-treated diabetic and nondiabetic hyperalgesic mice. DRG collected from control, STZ-treated diabetic mice, and nondiabetic mice 1 week after STZ or vehicle treatment were probed for TRPV1 and p-p38 MAPK by Western blots. Representative Western blots show elevated TRPV1 and p-p38 MAPK levels in diabetic and nondiabetic hyperalgesic mice. Summary graph shows -fold increase in TRPV1 and p-p38 MAPK levels calculated as a ratio of β-actin and total p38 MAPK levels, respectively. Asterisk represents the significance levels (*, $p < 0.05$ compared with control).

which adenine 5′-diphosphoribose is generated using cellular NAD^+ as a substrate (LeDoux et al., 1988; Delaney et al., 1995; Pieper et al., 1999). ADP-ribose is a potent activator of TRPMelastatin 2, which has been suggested to play a role in sensing oxidative stress (Fonfria et al., 2004).

Together, our results suggest that STZ exerts a direct action on neurons altering the expression and function of TRPV1 via the ROS-p38 MAPK pathway-mediated translational regulation. Of course, we cannot rule out the possibility that STZ might exert its effects on other nociceptive ion channels such as the voltage-gated sodium channels and the mechanosensitive channels. Therefore, future studies are needed to address the extent of modulation of other ion channels by direct action of STZ (Hayase et al., 2007). To our knowledge, this is the first report suggesting that STZ might have a direct effect on neurons; thus, caution should be exercised in interpreting data as diabetes- or hypoglycemia-induced while using STZ as a diabetogenic agent.

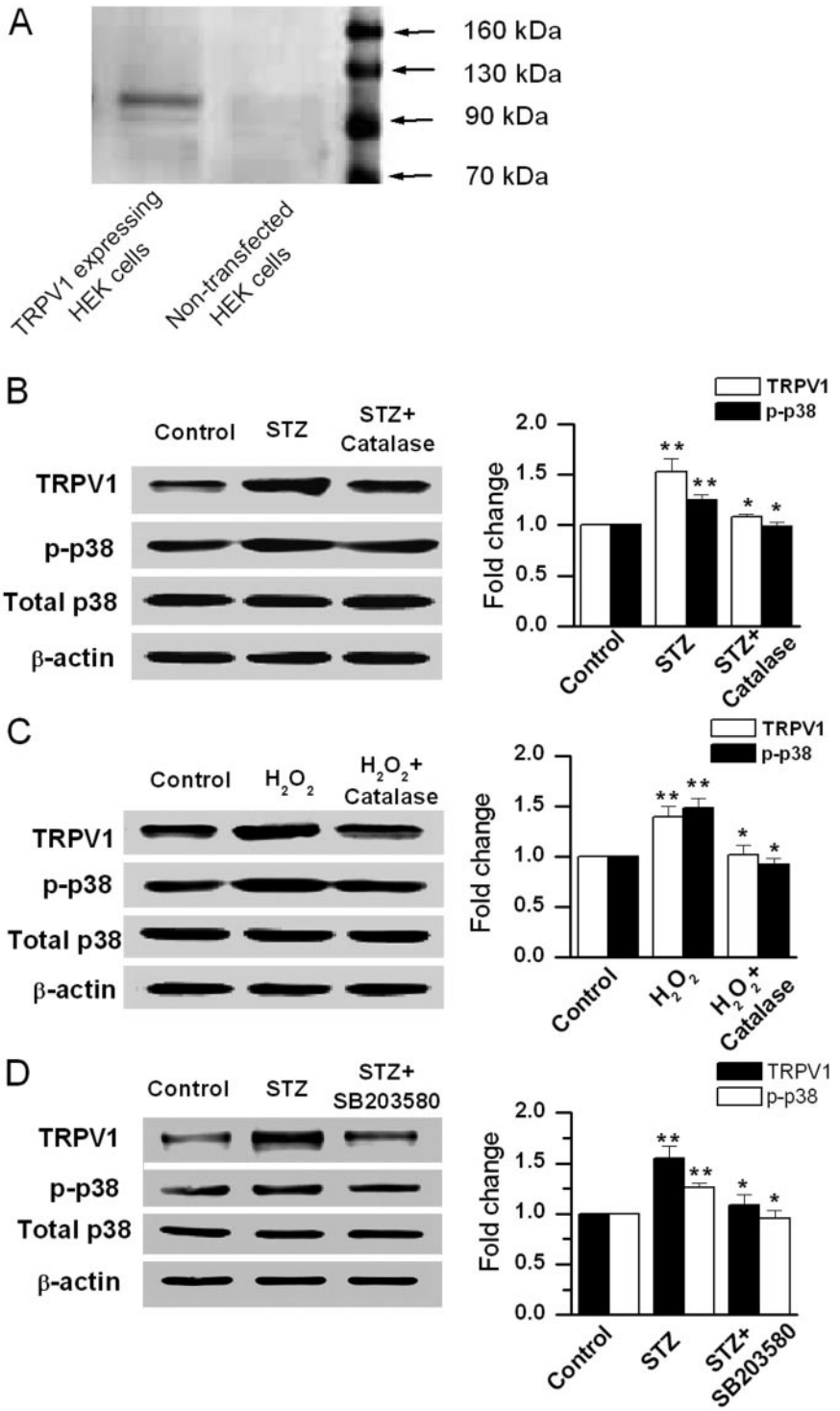

Fig. 8. STZ-induced increase in TRPV1 levels is mediated by ROS-p38 MAPK pathway. Stably TRPV1-transfected HEK 293T cells were treated with STZ (100 μM) or H_2O_2 (25 μM) and along with catalase or p38 MAPK inhibitor (SB203580) for 24 h, and Western blots were performed. A, TRPV1 expression in transfected HEK cells and no TRPV1 was detected in nontransfected HEK cells. B, STZ induced an increase in TRPV1 and p-p38 MAPK levels, which was blocked by concomitant treatment with catalase (200 U/ml). C, H_2O_2-induced increase in TRPV1, and p-p38 MAPK levels were blocked by treatment with catalase. D, STZ-induced increase in TRPV1 and p-p38 MAPK levels were blocked by treatment with a p38 MAPK inhibitor SB203580 (20 μM). Right, the summary graphs of TRPV1 and p-p38 MAPK levels. Asterisks represent the significance levels (*, $p < 0.05$ compared with STZ treatment; **, $p < 0.01$ compared with control).

MOL PHARM
MOLECULAR PHARMACOLOGY
aspet

Acknowledgments

The TRPV1 cDNA was kindly provided by David Julius (University of California, San Francisco, CA).

References

Abe J, Kusuhara M, Ulevitch RJ, Berk BC, and Lee JD (1996) Big mitogen-activated protein kinase 1 (BMK1) is a redox-sensitive kinase. *J Biol Chem* **271:**16586–16590.

Angel P and Karin M (1991) The role of jun, fos and the AP-1 complex in cell proliferation and transformation. *Biochim Biophys Acta* **1072:**129–157.

Berger NA (1985) Poly (ADP-ribose) in the cellular response to DNA damage. *Radiat Res* **101:**4–15.

Birder LA, Kanai AJ, De Groat WC, Kiss S, Nealan ML, Burke NE, Dineley KE, Watkins S, Reynolds IJ, and Caterina MJ (2001) Vanilloid receptor expression suggests a sensory role for urinary bladder epithelial cells. *Proc Natl Acad Sci U S A* **98:**13396–13401.

Brambilla G, Carlo P, Finollo R, and Sciaba L (1987) Dose-response curves for liver DNA fragmentation induced in rats by sixteen N-nitroso compounds as measured by viscometric and alkaline elution analyses. *Cancer Res* **47:**3485–3491.

Brussee V, Cunningham FA, and Zochodne DW (2004) Direct insulin signaling of neurons reverses diabetic neuropathy. *Diabetes* **53:**1824–1830.

Burkart V, Wang ZQ, Radons J, Heller B, Herceg Z, Stingl L, Wagner EF, and Kolb H (1999) Mice lacking the poly (ADP-ribose) polymerase gene are resistant to pancreatic beta-cell destruction and diabetes development induced by streptozocin. *Nat Med* **5:**314–319.

Caterina MJ, Leffler A, Malmberg AB, Martin WJ, Trafton J, Petersen-Zeitz KR, Koltzenburg M, Basbaum AI, and Julius D (2000) Impaired nociception and pain sensation in mice lacking the capsaicin receptor. *Science* **288:**306–313.

Caterina MJ, Schumacher MA, Tominaga M, Rosen TA, Levine JD, and Julius D (1997) The capsaicin receptor: a heat-activated ion channel in the pain pathway. *Nature* **389:**816–824.

Chen SR and Pan HL (2002) Hypersensitivity of spinothalamic tract neurons associated with diabetic neuropathic pain in rats. *J Neurophysiol* **87:**2726–2733.

Clapham DE (2003) TRP channels as cellular sensors. *Nature* **426:**517–524.

Courteix C, Bardin M, Massol J, Fialip J, Lavarenne J, and Eschalier A (1996) Daily insulin treatment relieves long-term hyperalgesia in streptozotocin diabetic rats. *Neuroreport* **7:**1922–1924.

Davis JB, Gray J, Gunthorpe MJ, Hatcher JP, Davey PT, Overend P, Harries MH, Latcham J, Clapham C, Atkinson K, et al. (2000) Vanilloid receptor-1 is essential for inflammatory thermal hyperalgesia. *Nature* **405:**183–187.

Delaney CA, Dunger A, Di Matteo M, Cunningham JM, Green MH, and Green IC (1995) Comparison of inhibition of glucose-stimulated insulin secretion in rat islets of Langerhans by streptozotocin and methyl and ethyl nitrosoureas and methane sulphonates. Lack of correlation with nitric oxide-releasing or O6-alkylating ability. *Biochem Pharmacol* **50:**2015–2020.

Devary Y, Gottlieb RA, Laus LF, and Karin M (1991) Rapid and preferential activation of the c-jun gene during the mammalian UV response. *Mol Cell Biol* **11:**2804–2811.

Fonfria E, Marshall IC, Benham CD, Boyfield I, Brown JD, Hill K, Hughes JP, Skaper SD, and McNulty S (2004) TRPM2 channel opening in response to oxidative stress is dependent on activation of poly(ADP-ribose) polymerase. *Br J Pharmacol* **143:**186–192.

Forst T, Pohlmann T, Kunt T, Goitom K, Schulz G, Lobig M, Engelbach M, Beyer J, and Pfutzner A (2002) The influence of local capsaicin treatment on small nerve fibre function and neurovascular control in symptomatic diabetic neuropathy. *Acta Diabetol* **39:**1–6.

Hayase F, Matsuura H, Sanada M, Kitada-Hamada K, Omatsu-Kanbe M, Maeda K, Kashiwagi A, and Yasuda H (2007) Inhibitory action of protein kinase Cbeta inhibitor on tetrodotoxin-resistant Na+ current in small dorsal root ganglion neurons in diabetic rats. *Neurosci Lett* **417:**90–94.

Hehner SP, Breitkreutz R, Shubinsky G, Unsoeld H, Schulze-Osthoff K, Schmitz ML, and Dröge W (2000) Enhancement of T cell receptor signaling by a mild oxidative shift in the intracellular thiol pool. *J Immunol* **165:**4319–4328.

Hong S and Wiley JW (2005) Early painful diabetic neuropathy is associated with differential changes in the expression and function of vanilloid receptor 1. *J Biol Chem* **280:**618–627.

Huang SM, Bisogno T, Trevisani M, Al-Hayani A, De Petrocellis L, Fezza F, Tognetto M, Petros TJ, Krey JF, Chu CJ, et al. (2002) An endogenous capsaicin-like substance with high potency at recombinant and native vanilloid VR1 receptors. *Proc Natl Acad Sci U S A* **99:**8400–8405.

Ji RR, Samad TA, Jin S, Schomll R, and Woolf CJ (2002) p38 MAPK activation by NGF in primary sensory neurons after inflammation increases TRPV1 levels and maintains heat hyperalgesia. *Neuron* **36:**57–68.

Johnston APW, Campbell JE, Found JG, Riddell MC, and Hawke TJ (2007) Streptozotocin induces G2 arrest in skeletal muscle myoblasts and impairs muscle growth in vivo. *Am J Physiol Cell Physiol* **292:**C1033–C1040.

Julius D and Basbaum AI (2001) Molecular mechanisms of nociception. *Nature* **413:**203–210.

Kamei J, Zushida K, Morita K, Sasaki M, and Tanaka S (2001) Role of vanilloid VR1 receptor in thermal allodynia and hyperalgesia in diabetic mice. *Eur J Pharmacol* **422:**83–86.

Kamei U, Ohhashi Y, Aoki T, and Kasuya Y (1991) Streptozotocin-induced diabetes in mice reduces the nociceptive threshold, as recognized after application of noxious mechanical stimuli but not of thermal stimuli. *Pharmacol Biochem Behav* **39:**541–544.

Konrad RJ, Mikolaenko I, Tolar JF, Liu K, and Kudlow JE (2001) The potential mechanism of the diabetogenic action of streptozotocin: inhibition of pancreatic beta-cell *O*-GlcNAc-selective *N*-acetyl-beta-D-glucosaminidase. *Biochem J* **356:**31–41.

Kröncke KD, Fehsel K, Sommer A, Rodriguez ML, and Kolb-Bachofen V (1995) Nitric oxide generation during cellular metabolization of the diabetogenic *N*-methyl-*N*-nitroso-urea streptozotocin contributes to islet cell DNA damage. *Biol Chem Hoppe Seyler* **376:**179–185.

LeDoux SP, Hall CR, Forbes PM, Patton NJ, and Wilson GL (1988) Mechanism of nicotinamide and thymidine protection from alloxan and streptozotocin toxicity. *Diabetes* **37:**1015–1019.

Lo D, Freedman J, Hesse S, Palmiter RD, Brinster RL, and Sherman LA (1992) Peripheral tolerance to an islet cell-specific hemagglutinin transgene affects both CD4+ and CD8+ T cells. *Eur J Immunol* **22:**1013–1022.

Luo ZD, Chaplan SR, Higuera ES, Sorkin LS, Stauderman KA, Williams ME, and Yaksh TL (2001) Upregulation of dorsal root ganglion $\alpha 2\delta$ calcium channel subunit and its correlation with allodynia in spinal nerve-injured rats. *J Neurosci* **21:**1868–1875.

Meyer M, Schreck R, and Baeuerle PA (1993) H_2O_2 and antioxidants have opposite effects on activation of NF-kB and AP-1 in intact cells: AP-1 as secondary antioxidant response factor. *EMBO J* **12:**2005–2015.

Mezey E, Toth ZE, Cortright DN, Arzubi MK, Krause JE, Elde R, Guo A, Blumberg PM, and Szallasi A (2000) Distribution of mRNA for vanilloid receptor subtype 1 (VR1), and VR1-like immunoreactivity, in the central nervous system of the rat and human. *Proc Natl Acad Sci U S A* **97:**3655–3660.

Nukatsuka M, Yoshimura Y, Nishida M, and Kawada J (1990) Allopurinol protects pancreatic beta cells from the cytotoxic effect of streptozotocin in vitro study. *J Pharmacobiodyn* **13:**259–262.

Petzold GL and Swenberg JA (1978) Detection of DNA damage induced in vivo following exposure of rats to carcinogens. *Cancer Res* **38:**1589–1594.

Pieper AA, Brat DJ, Krug DK, Watkins CC, Gupta A, Blackshaw S, Verma A, Wang ZQ, and Snyder SH (1999) Poly (ADP-ribose) polymerase-deficient mice are protected from streptozotocin-induced diabetes. *Proc Natl Acad Sci U S A* **96:**3059–3064.

Puntambekar P, Mukherjea D, Jajoo S, and Ramkumar V (2005) Essential role of Rac1/NADPH oxidase in nerve growth factor induction of TRPV1 expression. *J Neurochem* **95:**1689–1703.

Romanovsky D, Hastings SL, Stimers JR, and Dobretsov M (2004) Relevance of hyperglycemia to early mechanical hyperalgesia in streptozotocin-induced diabetes. *J Peripher Nerv Syst* **9:**62–69.

Schnedl WJ, Ferber S, Johnson JH, and Newgard CB (1994) STZ transport and cytotoxicity. Specific enhancement in GLUT2-expressing cells. *Diabetes* **43:**1326–1333.

Sofue M, Yoshimura Y, Nishida M, and Kawada J (1991) Uptake of nicotinamide by rat pancreatic beta cells with regard to streptozotocin action. *J Endocrinol* **131:**135–138.

Sugimoto K, Murakawa Y, and Sima AA (2000) Diabetic neuropathy a continuing enigma. *Diabetes Metab Res Rev* **16:**408–433.

Suzukawa K, Miura K, Mitsushita J, Resau J, Hirose K, Crystal R, and Kamata T (2000) Nerve growth factor-induced neuronal differentiation requires generation of Rac1-regulated reactive oxygen species. *J Biol Chem* **275:**13175–13178.

Turk J, Corbett JA, Ramanadham S, Bohrer A, and McDaniel L (1993) Biochemical evidence for nitric oxide formation from streptozotocin in isolated pancreatic islets. *Biochem Biophys Res Commun* **197:**1458–1464.

Zhou XF, Chie ET, Deng YS, Zhong JH, Xue Q, Rush RA, and Xian CJ (1999) Injured primary sensory neurons switch phenotype for brain-derived neurotrophic factor in the rat. *Neuroscience* **92:**841–853.

Zhuang HX, Wuarin L, Fei ZJ, and Ishii DN (1997) Insulin-like growth factor (IGF) gene expression is reduced in neural tissues and liver from rats with non-insulin-dependent diabetes mellitus, and IGF treatment ameliorates diabetic neuropathy. *J Pharmacol Exp Ther* **283:**366–374.

Address correspondence to: Dr. Louis S. Premkumar, Department of Pharmacology, Southern Illinois University School of Medicine, Springfield, IL 62702. E-mail: lpremkumar@siumed.edu